Single-molecule tracking-based drug screening

Authors: Daisuke Watanabe[1,2], Michio Hiroshima[1,2,3]*, Masahiro Ueda[1,2]*

Affiliations:

[1]Laboratory of Single Molecule Biology, Department of Biological Sciences, Graduate School of Science, Osaka University; Toyonaka, Osaka, Japan.

[2]Laboratory for Cell Signaling Dynamics, Center for Biosystems Dynamics Research, RIKEN; Suita, Osaka, Japan.

[3]Cellular Informatics Laboratory, Cluster for Pioneering Research, RIKEN; Wako, Saitama, Japan.

*Corresponding authors.

Email: m_hiroshima.fbs@osaka-u.ac.jp and ueda.masahiro.fbs@osaka-u.ac.jp.

Abstract:

The single-molecule tracking of transmembrane receptors in living cells has provided significant insights into signaling mechanisms, such as mobility and clustering upon their activation/inactivation, making it a potential screening method for drug discovery. Using an automated system for large-scale single-molecule analysis, we screened for epidermal growth factor receptor (EGFR) from 1,134 of FDA approved drugs. Included in the hit 18 compounds covered all EGFR-targeted tyrosine kinase inhibitors in the library that suppressed phosphorylation-dependent mobility shift of EGFR, proving the concept of this approach. The remaining hit compounds are not reported as EGFR-targeted drugs and affected the mobility and/or clustering of EGFR to prevent EGFR-dependent cell growth. Thus, single-molecule tracking provides a new modality for discovering novel therapeutics on various receptor functions with previously untargeted mechanisms.

Main Text:

Transmembrane receptors trigger signal transduction in cells to induce cellular responses. Since the downstream signaling depends on the functional properties of receptors, various diseases are often attributed to receptor dysfunction. In drug discovery, the largest number of target molecules are membrane receptors (> 50% of total), such as receptor tyrosine kinases (RTKs), G protein-coupled receptors (GPCRs), and immune receptors, followed by nuclear receptors (< 20%) (*1–3*). Epidermal growth factor receptor (EGFR), an RTK, mediates signal transduction for cell proliferation, differentiation, migration, and apoptosis, and is a primary target molecule in drug exploration because its overexpression and/or mutations are found in various types of cancer cells (*4–7*). Many small-molecule drugs against a well-known EGFR-related cancer, non-small cell lung cancer (NSCLC), have been developed: gefitinib, erlotinib, and icotinib as first-generation tyrosine kinase inhibitors (TKIs); afatinib and dacomitinib as second-generation TKIs; and osimertinib as third-generation (*8*). These drugs have been evaluated by their inhibitory effects on tyrosine kinase activity (*9*), but EGFR undergoes multiple signaling processes including tyrosine phosphorylation, oligomerization, coupling with adaptor molecules and internalization (*10*). In general, assays for drug discovery focus on a particular step in the signaling pathway exhibited by the targeting molecules. However, assays that select for compounds that have effects on multiple steps in the signaling pathway are of interest because of their different mechanisms of action on the same target (*11*).

Single-molecule imaging analysis has been used to visualize and measure the location and brightness of individual molecules in cells (*12–14*). These measurements provide information on the lateral diffusion and oligomerization/clustering of receptors on the membrane of living cells. In the case of EGFR, the behavioral transition on the membrane, which is described by EGFR mobility and clustering dynamics, has been shown to correlate to the signaling process: EGF

triggers tyrosine phosphorylation, leading to the translocation of EGFR along the membrane to a specific region where the mobility of EGFR is confined and the clusters responsible for downstream signaling are formed, followed by internalization into endosomes. Single-molecule imaging has also revealed other processes during EGFR signaling, such as ligand-receptor binding kinetics, molecular structure transitions depending on membrane components, and colocalization with receptors for different signaling pathways (*15–19*). That is, single-molecule imaging can analyze multiple events during a series of EGFR signaling processes. Although this technique is powerful for understanding molecular mechanisms and evaluating the effects of pharmacological compounds, its low throughput for data acquisition arising from its expertise- and manual-dependent processes prevents it from being employed for large-scale analysis. As a solution, we previously developed a fully automated, in-cell single-molecule imaging system equipped with robotics and machine learning (AiSIS) (*20*) that has a 100-fold higher throughput than standard single-molecule analysis techniques. High throughput methods like AiSIS detect simultaneously various events occurring during the signaling process of the target molecule, allowing researchers to explore drugs with different mechanisms of action on the target molecule.

Here, we use these techniques to screen for compounds targeting transmembrane receptors. To prove the concept of this approach, we screened for EGFR from a library consisting of 1,134 FDA approved compounds and successfully selected all tyrosine kinase inhibitors contained in the library. Furthermore, the other hit compounds exhibited effects in the clustering, internalization, and expression level of EGFR without any significant inhibition of the tyrosine kinase activity upon EGF stimulation. Different from screening methods that focus on a single event in the molecular process, our method could assess the various events occurring during the signal transduction of the target molecule.

Results

EGFR mobility-based screening

AiSIS allows for a large-scale, single-molecule analysis using 96-well plates (Fig. 1A). Cells in each well were treated with a compound, and single-molecule imaging using total internal reflection fluorescence microscopy (TIRFM) was automatically executed well by well. The field of views suitable for the single-molecule analysis were determined by machine learning-based automated cell searching. During the imaging, autofocusing was continuously running, and the ligand was dispensed at desired times by robotics. This system measured 400 cells per hour, which corresponds to 9,000 - 10,000 cells per day, and included approximately 100 million molecules. Fig. 1B shows a single EGFR-mEGFP complex expressed in CHO-K1 cells, which lack endogenous EGFR. From the images acquired under optimized conditions (table S1), trajectory data, including the positions and brightness of fluorescent EGFR, were obtained by single-molecule tracking (Fig. 1C) and used to quantify the mobility of EGFR with diffusion coefficients and mean square displacements (MSD) (Fig. 1D and table S2). The mobility decreased with EGF addition, as shown by the MSD (Fig. 1D, top), consistent with a previous study (*20*). This EGF-induced mobility shift was recovered by treatment with a TKI (gefitinib, Fig. 1D, bottom), which confirmed EGFR mobility tightly correlated with EGF-activated kinase function. As shown in Fig. 1E, a linear relationship was found between the changes in MSD measured every 500 ms (MSD_{500ms}) and EGFR phosphorylation under various EGF concentrations. The inhibitory effects of gefitinib on EGF-induced decrease of MSD_{500ms} are shown in Fig. 1F (top). Because TKI itself seems to have little effect on the mobility in our data, the MSD ratio (MSD with EGF to MSD without EGF) was used to evaluate the compounds en bloc. As shown in Fig. 1F (bottom), when the EGF concentration was 30 nM, the ratio was

approximately 0.2 for untreated cells but approached 1 for treated cells due to suppression of the EGF-induced decrease of EGFR mobility.

We extended the single-molecule tracking-based assay to drug screening. First, we optimized the conditions of the image acquisition (fig. S1), and the suitability of this approach as a screening method was assessed using the indices calculated from MSD_{500ms}, with the positive control being cells treated with gefitinib and EGF and the negative control being cells treated only with EGF (Fig. 2A). The coefficient of variation (CV), signal/background (S/B), and Z'-factor were respectively defined as the ratio of the standard deviation (SD) and average of the controls, as the ratio between the averages of the positive (signal) and negative (background) controls, and as the following equation:

$$Z' = \left(3 \times SD_{positive} + 3 \times SD_{negative}\right) \Big/ \left(Avg_{positive} - Avg_{negative}\right) \qquad \text{Eq. (1)}$$

, where $SD_{\mathbf{positive}}$, $SD_{negative}$, $Avg_{\mathbf{positive}}$, and $Avg_{negative}$ represent SD and average for the positive and negative controls, respectively. The obtained indices for our system were 4% for CV, 2.7% for S/B, and 0.64 for Z'-factor. All these values were shown to satisfy the thresholds of ≤ 10% for CV, ≥ 2% for SB, and ≥ 0.50 for Z'-factor for drug screening. Next, we carried out the screening using a library of 1,134 FDA-approved compounds whose target proteins are responsible for broad functions such as receptors, channels, kinases, enzymes, transporters, and so on (Fig. 2B). This library includes 7 marketed drugs that act as TKI for EGFR (afatinib, erlotinib, OSI-420 (the active metabolite of erlotinib), gefitinib, lapatinib, lapatinib ditosylate (another form of lapatinib), and vandetanib). To explore compounds significantly affecting EGFR mobility, the screening procedure was designed as follows: 1) cultured cells in each well of a 96-well plate were pretreated with 100 μL of 10 μM compound solution at 37°C for 1 hour, 2) single-molecule imaging was automatically done on 20 different cells, 3) 100 μL of 120 nM

EGF solution was added by the automatic dispenser so that the final concentration of EGF was 60 nM, and 4) another 20 cells were imaged 1.5 min after the EGF addition. During the screening, the Z'-factor was calculated for every assay plate from positive- and negative-control wells (20 cells in each well) to evaluate the screening quality, and images acquired from the plates passing the quality inspection were used in the following analysis. For each compound, when the MSD_{500ms} ratio was beyond the average + 3 SD of the MSD_{500ms} ratio for the negative control, the compound was regarded as causing a significant MSD change of EGFR and identified as a hit compound. Fig. 2C shows the selected 53 compounds with MSD_{500ms} ratios for compounds normalized to the negative control ratio. One of the marketed EGFR-targeted drugs, genistein, which is a flavonoid and known to inhibit tyrosine kinases including EGFR, was excluded due to its IC_{50} (50% inhibitory concentration) being above 10 μM, which was beyond our experimental condition.

For a more detailed assessment of the selected 53 compounds, we measured the dose-dependent effects of the compounds on EGFR mobility with and without EGF (fig. S2). Compounds with significantly different MSD values at the minimum and maximum concentrations were selected. A threshold was defined as the half of the difference between the MSD (averaged over ~30 cells) at the two concentrations exceeding the sum of their standard deviations. As a result, 18 compounds were obtained, but one of them, auranofin, was excluded from further analysis due to its cytotoxicity (cell death) during the treatment. Although these compounds showed similarly high MSD ratios, we found two types of effects on the MSD: one changed the receptor mobility primarily after the EGF addition (Fig. 2D), and the other before the addition (Fig. 2E). Among the 17 compounds, 10 compounds corresponded to the former case and suppressed the EGF-dependent decrease in a dose-dependent manner (Fig. 2D). These 10 were all kinase inhibitors: afatinib, erlotinib, OSI-420, gefitinib, lapatinib, and lapatinib

ditosylate are known as EGFR-TKIs (*8*, *21*); ponatinib and vandetanib are pan-TKIs (*22*); and dasatinib and ibrutinib have been reported as Bruton's tyrosine kinase inhibitors (*23*) and can interfere with EGFR phosphorylation. All these EGFR-TKIs in the library were hit compounds (table S3), proving that our method was valid for exploring drugs targeting tyrosine phosphorylation of the receptor.

The other 7 hit compounds affected another function of EGFR and did not affect the EGF-induced decrease in mobility (Fig. 2E). The reported drug actions and approved applicable symptoms are not apparently concerned with the EGFR tyrosine kinase: broxyquinoline is an anti-infective agent; daunorubicin is an anthracycline antibiotic used for chemotherapeutic agents against cancer by inhibiting DNA topoisomerase II (*24*); eltrombopag is used to treat severe aplastic anemia and activates thrombopoietin receptor (TPOR) to facilitate platelet production (*25*); glafenine is a non-steroidal anti-inflammatory drug (NSAID) that inhibits cyclooxygenase-2/prostaglandin E2 (COX-2/PGE2) signaling (*26*); nilotinib and sorafenib are not EGFR-TKI but TKI that largely inhibit EGFR-independent pathways and used to respectively to treat primary kidney cancer (*27*) and chronic myeloid leukemia (*28*); and, finally, curcumin interferes with tyrosine kinases including EGFR and was approved as a food additive. Because these compounds induced EGFR mobility changes without EGF, they are suggested to interact directly or indirectly with EGFR by some actions other than the inhibition of tyrosine kinase. The effects of these compounds on EGFR are described in more detail below.

EGFR clustering-based screening

Single-molecule tracking can obtain the brightness of each EGFR-GFP fluorescent spot, which reflects the number of GFP involved. Because CHO-K1 cells express no endogenous EGFR, their brightness reflects the oligomer/clustering size. The EGF concentration correlated with the

brightness (Fig. 3A and B), indicating that monomers/dimers were relatively reduced with increasing concentration and larger size clusters were gained. The formation of clusters with integrating monomers/dimers has been suggested to corelate with the activation of downstream signaling through interactions with adaptor molecules (*15*). Thus, the increase in brightness could be used as a screening index to assess signal transduction.

For the obtained single-molecule tracking data, we compared the probability density distributions of the spot brightness before and after compound treatment without EGF. The Kullback-Leibler divergence (KLD) was used to quantify the similarity of the histogram profiles. In this case, Z'-factors were calculated using KLD before and after the EGF addition (without any compound) as respective negative and positive controls. The observed Z'-factors did not satisfy the threshold of 0.5 due to the broad SD (fig. S3). Nevertheless, the highest KLD value among the compounds (Fig. 3C) was obviously different from the KLD calculated for the negative control. This compound, verteporfin, diminished the number of brighter spots in a dose-dependent manner (Fig. 3, D to F), indicating that large oligomers were disassembled to dimers or monomers. Verteporfin is a photosensitizing drug for age-related macular degeneration (*29*).

Characterization of hit compounds on EGFR dynamics, signal transduction and cell viability

To further characterize the hit compounds, we obtained two-dimensional (2D) probability density heatmaps of EGFR molecules from MSD_{30ms} and brightness data of individual EGFR spots, which we defined by the mobility and clustering in the *y*- and *x*-axes, respectively (Fig. 4A and fig. S4). In the case of untreated cells, EGF stimulation induced transitions towards a slower mobility and larger clusters, which can be seen in the differential heatmaps between with and without EGF (Fig. 4A, no compound). For EGFR-TKI-treated cells, the EGF-induced transition

was reduced, indicating an inhibition of changes in mobility and clustering with EGFR-TKI (Fig. 4A, tyrosine kinase inhibitor, and fig. S4A). In this case, after the EGF addition, EGFR mobility in EGFR-TKI-related cells was larger than in untreated cells, demonstrating the kinase activity-dependent mobility shift of EGFR. When treated with non-EGFR-TKI compounds affecting EGFR mobility, such as eltrombopag, the transition to slower mobility occurred without EGF addition (Fig. 4A, compounds affecting mobility, and fig. S4B). In the case of verteporfin, which changes the clustering of EGFR, a transition to smaller clusters and moderate shift to slower mobility was observed (Fig. 4A, compounds affecting clusters). Thus, the obtained compounds affect the mobility and/or clustering of EGFR depending on the compound type, suggesting different actions on EGFR.

We evaluated the effects of the hit compounds on the cellular viability (except for derivatives of erlotinib and lapatinib, and curcumin which is not a drug but a food additive). Viability assays of A431 and CHO-K1 cells, which endogenously express and do not express EGFR, respectively, were carried out under 10 μM compounds for 72 hours. All the hit EGFR-TKIs (i.e. afatinib, erlotinib, gefitinib, lapatinib, ponatinib, vandetanib, dasatinib and ibrutinib) reduced the viability of A431 cells but did not change the viability of CHO-K1 cells (Fig. 4B), consistent with A431 cells depending on EGFR activity for their survival (*30*). That is, all the hit EGFR-TKIs that inhibited the phosphorylation-dependent mobility shift of EGFR upon EGF stimulation reduced the EGFR-dependent viability of A431 cells, probably due to inhibition of the kinase activity. Among the 6 non-EGFR-TKI compounds that decreased EGFR mobility without EGF, 4 compounds (broxyquinoline, daunorubicin, eltrombopag, and sorafenib) reduced the viability of A431 cells but not of CHO-K1 cells, meaning that these compounds may affect EGFR-dependent signaling processes for cell survival, while the other two compounds (glafenine and nilotinib) did not alter the viability of either cell type, suggesting no effects on EGFR-dependent

cell viability. Verteporfin, the non-EGFR-TKI compound effective for EGFR clustering, also decreased the viability of A431, similar to the above 4 compounds. Thus, all EGFR-TKIs inhibited EGFR-dependent cell growth, but the 7 non-EGFR-TKI compounds were diverse in their effects on cell growth.

Next, we investigated whether these non-EGFR-TKI compounds affect EGFR-dependent signaling. The activation and expression level of signaling proteins were examined in A431 cells (Fig. 4, C to E). The treatment of five non-EGFR-TKI compounds (broxyquinoline, daunorubicin, eltrombopag, sorafenib, and verteporfin) showed no significant inhibition in EGFR phosphorylation upon EGF stimulation in comparison with the control (untreated) condition (Fig. 4D), consistent with these compounds not being EGFR-TKIs. The total amount of EGFR in A431 cells decreased following treatment with non-EGFR-TKI compounds except for sorafenib (Fig. 4E), showing the destabilization of EGFR. In the subsequent signaling, the phosphorylation of a downstream protein, ERK, fell significantly by treatment with the five compounds that reduced the viability, although the expression levels of ERK were not affected. Furthermore, EGFR internalization occurred in the cells treated with the five compounds without EGF, as shown in timelapse TIRF images (Fig. 4F) and by quantification (Fig. 4G, left). On the other hand, when treated with the other two non-EGFR-TKI compounds, glafenine and nilotinib, which had no effect on cell viability, the cells exhibited normal EGF-induced EGFR phosphorylation and downstream proteins (Fig. 4D) and showed no EGFR internalization (Fig. 4G, right). Thus, the five non-EGFR-TKI compounds (broxyquinoline, daunorubicin, eltrombopag, sorafenib, and verteporfin) that reduced EGFR-dependent cell viability caused the downregulation of EGFR-related signal transduction with internalization, even though EGFR phosphorylation was unchanged. That is, compounds that can alter EGFR signaling outside

tyrosine phosphorylation were successfully selected by the single-molecule tracking-based screening method.

Discussion

Here, we demonstrated single-molecule tracking-based drug screening to explore compounds effective against EGFR. This method observed changes in EGFR mobility and clustering instead of focusing on a specific process of the signaling, allowing it to detect changes in multiple processes dependent on the ligand. Our screening widely selected compounds affecting EGFR functions related and unrelated to EGF stimulation (Fig. 2C). Among the hit compounds, those suppressing the EGF-induced mobility shift of EGFR (Fig. 2D) were identified as EGFR-TKIs. Accumulating evidence shows that EGFR undergoes structural changes during its phosphorylation upon EGF stimulation and then translocates to a confined membrane region via interactions with membrane components (lipid, proteins, etc.), leading to slower receptor mobility (*15*). Changes in the MSD of EGFR were proven to couple tightly with the phosphorylation in a dose-dependent manner (Fig. 1E). The competitive docking of TKI to the ATP-binding pocket of EGFR prevents the receptor from subsequent structural changes during phosphorylation, which thus suppresses the decrease in mobility and subsequent signaling processes (Fig. 5A). This is one of the possible reasons why EGFR-targeted TKIs can be detected by the mobility-based screening.

In addition, our screening detected the reduced mobility of EGFR upon treatment with several hit compounds without EGF (i.e. broxyquinoline, daunorubicin, eltrombopag, sorafenib, glafenine, and nilotinib), none of which are known to act on EGFR directly. Some compounds were reported to interact with the plasma membrane to possibly alter EGFR mobility: daunorubicin presents cytotoxic effects by penetrating the membrane (*31*), eltrombopag binds to the transmembrane region of TpoR (*32*), and broxyquinoline introduces oxygen free radicals into the membrane. On the other hand, mechanisms involving more direct interactions with EGFR to reduce the mobility are suggested from the previous reports (*33–36*). Fig. 5B shows possible

schemes for how broxyquinoline, daunorubicin, eltrombopag, and sorafenib showed the following effects; these compounds commonly reduced mobility (Fig. 2E), suppressed downstream signaling (Fig. 4D), facilitated internalization (Fig. 4, F and G) and decreased EGFR expression levels (Fig. 4E). We assume that these compounds force EGFR to form a protein complex with other proteins in a specific membrane subdomain where receptor mobility is lower. The candidate proteins in the complex that interact with these compounds are as follows. Broxyquinoline stabilizes hypoxia inducible factor (HIF)-1 (*33*) to acutely accumulate caveolin-1 in the lipid raft to constitute caveolae (*34*), which directly interacts with EGFR and confines protein mobility. Daunorubicin generates reactive oxygen species (ROS) to stabilize HIF-1 (*35*), enabling a similar effect as broxyquinoline. Eltrombopag stabilizes syndecan (SCD)-4 (*36*), which can form a protein complex with EGFR and integrin $\alpha_5\beta_1$ (*37*). Sorafenib inhibits the kinase activity and induces the internalization of platelet-derived growth factor receptor (PDGFR)-β, which also can form a protein complex with EGFR, integrin $\alpha_5\beta_1$, and caveolin-1 (*38*). These complexes containing EGFR in the membrane subdomains have been reported to be internalized with caveolin-mediated endocytosis for broxyquinoline, daunorubicin, and sorafenib (*39*, *40*). Micropinocytosis with the enhancement of SDC-4 signaling has been shown for eltrombopag (*36*). The internalization exerts a harmful effect on the cell viability by inhibiting EGFR signaling for proliferation and survival (*41*). Fig. 5C illustrates how glafenine and nilotinib reduce EGFR mobility (Fig. 2D). Glafenine inhibits the activity of ATP-binding cassette transporter G2 (ABCG2) (*42*), while nilotinib targets PDGFR-α (*43*). However, interactions with EGFR by either ABCG2 or PDGFR-α have not been reported. At the same time, several studies have suggested that ABCG2 (*44*) and PDGFR-α (*45*) localize in a cholesterol rich region of the plasma membrane, plausibly affecting the mobility of adjacent receptors. No significant change was observed in the EGFR-dependent viability of cells treated

by these two compounds (Fig. 4B). Additionally, the phosphorylation of downstream proteins was not suppressed (Fig. 4, D and E) and no internalization/reduction of EGFR expression occurred (Fig. 4, E to G), indicating no downregulation of EGFR signaling. Finally, verteporfin (Fig. 5D), which is a photosensitizing drug for age-related macular degeneration, was selected by its significant decrease of the cluster size, as reflected in the fluorescent brightness (Fig. 3, C to E), but it was not a hit in mobility-based screening. Verteporfin downregulated EGFR signaling (Fig. 4D) and caused quick internalization (Fig. 4, F and G), consistent with a previous report (*46*) in which verteporfin inhibited anoctamin (ANO), a calcium–activated chloride channel that has stabilizing and activating functions for EGFR (*47*). The downregulation of EGFR signaling by verteporfin consequently reduces cell viability.

The hit compounds obtained were categorized into four types based on the observed EGFR behavior and cell responses, with each type suggested to depend on a different mechanism of action. The schemes in Fig. 5B and 5D would be effective for removing pathogenic cells that excessively express EGFR, a common phenotype of various cancers, by inducing cell death following EGFR internalization. Therefore, drug repositioning for novel EGFR drugs may be possible using compounds that exhibit these schemes. Our evaluation process covered all the schemes in Fig. 5 and thus incorporate various signaling processes into the screening. Besides EGFR, various types of receptors on the plasma membrane have been reported to change the mobility according to their activation and the cluster formation to propagate downstream signaling (*15*, *48–50*), suggesting that single-molecule analysis is applicable to a wide variety of membrane receptors. Beyond the existing screening framework, single-molecule tracking-based screening can explore compounds undetectable by conventional methods for various functions of disease-related receptors.

References and Notes

1. R. Santos, O. Ursu, A. Gaulton, A. P. Bento, R. S. Donadi, C. G. Bologa, A. Karlsson, B. Al-Lazikani, A. Hersey, T. I. Oprea, J. P. Overington, A comprehensive map of molecular drug targets. *Nat. Rev. Drug Discov.* **16**, 19–34 (2016).

2. A. L. Hopkins, C. R. Groom, The druggable genome. *Nat. Rev. Drug Discov.* **1**, 727–730 (2002).

3. S. Vasaikar, P. Bhatia, P. G. Bhatia, K. C. Yaiw, Complementary approaches to existing target based drug discovery for identifying novel drug targets. *Biomedicines*. **4**, 27 (2016).

4. T. Kovacs, F. Zakany, P. Nagy, It Takes More than Two to Tango : Complex , Hierarchal , and Membrane-Modulated Interactions in the Regulation of Receptor Tyrosine Kinases. *Cancers (Basel).* **14**, 944 (2022).

5. N. Normanno, M. R. Maiello, A. D. E. Luca, Epidermal Growth Factor Receptor Tyrosine Kinase Inhibitors (EGFR-TKIs): Simple Drugs With a Complex Mechanism of Action ? *J. Cell. Physiol.* **19**, 13–19 (2002).

6. M. Roengvoraphoj, G. J. Tsongalis, K. H. Dragnev, J. R. Rigas, Epidermal growth factor receptor tyrosine kinase inhibitors as initial therapy for non-small cell lung cancer: Focus on epidermal growth factor receptor mutation testing and mutation-positive patients. *Cancer Treat. Rev.* **39**, 839–850 (2013).

7. M. Chiba, Y. Togashi, E. Bannno, Y. Kobayashi, Y. Nakamura, H. Hayashi, M. Terashima, M. A. De Velasco, K. Sakai, Y. Fujita, T. Mitsudomi, K. Nishio, Efficacy of irreversible EGFR-TKIs for the uncommon secondary resistant EGFR mutations L747S, D761Y, and T854A. *BMC Cancer*. **17**, 281 (2017).

8. X. Du, B. Yang, Q. An, Y. G. Assaraf, X. Cao, J. Xia, X. Du, B. Yang, Q. An, Y. G. Assaraf, X. Cao, J. Xia, Acquired resistance to third-generation EGFR-TKIs and emerging next-generation EGFR inhibitors Acquired resistance to third-generation EGFR-TKIs and emerging next-generation EGFR inhibitors. *Innov.* **2**, 100103 (2021).

9. J. Gao, J. Jian, Z. Jiang, A. Van Schepdael, Screening assays for tyrosine kinase inhibitors : A review. *J. Pharm. Biomed. Anal.* **223**, 115166 (2023).

10. P. Wee, Z. Wang, Epidermal growth factor receptor cell proliferation signaling pathways. *Cancers (Basel).* **9**, 52 (2017).

11. C. Peters, D. Bascuñán, C. F. Burgos, C. Bobadilla, J. González-Sanmiguel, S. Boopathi, N. Riffo, E. J. Fernández-Pérez, M. E. Tarnok, L. F. Aguilar, W. Gonzalez, L. G. Aguayo, Characterization of a new molecule capable of inhibiting several steps of the amyloid cascade in Alzheimer's disease. *Neurobiol. Dis.* **141**, 104938 (2020).

12. Y. Sako, S. Minoguchi, T. Yanagida, Single-molecule imaging of EGFR signalling on the surface of living cells. *Nat. Cell Biol.* **2**, 168–72 (2000).

13. M. Ueda, Y. Sako, T. Tanaka, P. Devreotes, T. Yanagida, Single-molecule analysis of chemotactic signaling in Dictyostelium cells. *Science*. **294**, 864–7 (2001).

14. R. Iino, I. Koyama, a Kusumi, Single molecule imaging of green fluorescent proteins in living cells: E-cadherin forms oligomers on the free cell surface. *Biophys. J.* **80**, 2667–77 (2001).

15. M. Hiroshima, C. Pack, K. Kaizu, K. Takahashi, M. Ueda, Y. Sako, Transient Acceleration of Epidermal Growth Factor Receptor Dynamics Produces Higher-Order Signaling Clusters. *J. Mol. Biol.* **430**, 1386–1401 (2018).

16. Y. Teramura, J. Ichinose, H. Takagi, K. Nishida, T. Yanagida, Y. Sako, Single-molecule analysis of epidermal growth factor binding on the surface of living cells. *EMBO J.* **25**, 4215–22 (2006).

17. D. T. Clarke, M. L. Martin-fernandez, A Brief History of Single-Particle Tracking of the Epidermal Growth Factor Receptor (2019), doi:10.3390/mps2010012.

18. H. K. Byeon, Beyond EGFR inhibition : multilateral combat strategies to stop the progression of head and neck cancer. *Exp. Mol. Med.* **51**, 8 (2019).

19. M. C. Gamble, B. R. Williams, N. Singh, L. Posa, Z. Freyberg, R. W. Logan, S. Puig, Mu-opioid receptor and receptor tyrosine kinase crosstalk: Implications in mechanisms of opioid tolerance, reduced analgesia to neuropathic pain, dependence, and reward. *Front. Syst. Neurosci.* **16**, 1059089 (2022).

20. M. Yasui, M. Hiroshima, J. Kozuka, Y. Sako, M. Ueda, Automated single-molecule imaging in living cells. *Nat. Commun.* **9**, 3061 (2018).

21. M. A. S. Abourehab, A. M. Alqahtani, B. G. M. Y. Gouda, A. M. Gouda, Globally Approved EGFR Inhibitors: Insights into Their Syntheses, Target Kinases, Biological Activities, Receptor Interactions, and Metabolism. *Molecules*. **26**, 6677 (2021).

22. V. De Falco, P. Buonocore, M. Muthu, L. Torregrossa, F. Basolo, M. Billaud, J. M. Gozgit, F. Carlomagno, O. Sperimentale, Ponatinib (AP24534) Is a Novel Potent Inhibitor of Oncogenic RET Mutants Associated With Thyroid Cancer. *J Clin Endocrinol Metab*. **98**, 811–819 (2013).

23. R. E. Joseph, N. Amatya, D. B. Fulton, J. R. Engen, T. E. Wales, A. Andreotti, Differential impact of BTK active site inhibitors on the conformational state of full-length BTK. *Elife*. **9**, e60470 (2020).

24. M. Lehmann, K. De Souza, P. Vilar, A. Franco, R. De Andrade, Activity of Topoisomerase Inhibitors Daunorubicin, Idarubicin, and Aclarubicin in the Drosophila Somatic Mutation and Recombination Test. *Environ. Mol. Mutagen.* **257**, 250–257 (2004).

25. J. D. Grainger, Eltrombopag for the treatment of aplastic anemia : current perspectives. *Drug Des. Devel. Ther.* **10**, 2833–2843 (2016).

26. G. W. Carlile, Q. Yang, E. Matthes, J. Liao, V. Birault, H. F. Sneddon, D. L. Poole, C. J. Hall, J. W. Hanrahan, D. Y. Thomas, The NSAID glafenine rescues class 2 CFTR mutants via cyclooxygenase 2 inhibition of the arachidonic acid pathway. *Sci. Rep.* **12**, 4595 (2022).

27. C. Guevremont, C. Jeldres, P. Perrotte, P. I. Karakiewicz, Sorafenib in the management of metastatic renal cell carcinoma. *Curr. Oncol.* **16**, S27–S32 (2009).

28. H. M. Kantarjian, F. J. Giles, K. N. Bhalla, J. Pinilla-Ibarz, R. A. Larson, N. Gattermann, O. G. Ottmann, A. Hochhaus, J. P. Radich, G. Saglio, T. P. Hughes, G. Martinelli, D. W. Kim, Y. Shou, N. J. Gallagher, R. Blakesley, M. Baccarani, J. Cortes, P. D. Le Coutre, Nilotinib is effective in patients with chronic myeloid leukemia in chronic phase after imatinib resistance or intolerance: 24-month follow-up results. *Blood*. **117**, 1141–1145 (2011).

29. N. Borodoker, R. F. Spaide, L. Maranan, J. A. Sorenson, L. A. Yannuzzi, D. R. Guyer, Verteporfin Infusion-associated Pain. *Am J Ophthalmol*. **133**, 211–214 (2002).

30. M. L. Janmaat, F. A. E. Kruyt, J. A. Rodriguez, G. Giaccone, Response to epidermal growth factor receptor inhibitors in non-small cell lung cancer cells: Limited antiproliferative effects and absence of apoptosis associated with persistent activity of extracellular signal-regulated kinase or Akt kinase pathways. *Clin. Cancer Res.* **9**, 2316–2326 (2003).

31. A. C. Alves, D. Ribeiro, M. Horta, J. L. F. C. Lima, C. Nunes, S. Reis, A biophysical approach to daunorubicin interaction with model membranes: Relevance for the drug's biological activity. *J. R. Soc. Interface*. **14**, 20170408 (2017).

32. E. E. Matthews, D. Thévenin, J. M. Rogers, L. Gotow, P. D. Lira, L. A. Reiter, W. H. Brissette, D. M. Engelman, Thrombopoietin receptor activation: transmembrane helix dimerization, rotation, and allosteric modulation. *FASEB J.* **25**, 2234–2244 (2011).

33. S. Y. Kim, M. J. Lee, J. W. Kim, Y. R. Na, H. Y. Lee, H. Cho, K. B. Lee, Y. M. Lee, C. Lee, H. Park, E. G. Yang, Effects of clioquinol analogues on the hypoxia-inducible factor pathway and intracelullar mobilization of metal ions. *Biol. Pharm. Bull.* **35**, 2160–2169 (2012).

34. Y. Wang, O. Roche, C. Xu, E. H. Moriyama, P. Heir, J. Chung, F. C. Roos, Y. Chen, G. Finak, M. Milosevic, B. C. Wilson, B. T. Teh, M. Park, M. S. Irwin, M. Ohh, Hypoxia promotes ligand-independent EGF receptor signaling via hypoxia-inducible factor-mediated upregulation of caveolin-1. *Proc. Natl. Acad. Sci. U. S. A.* **109**, 4892–4897 (2012).

35. S. Y. Wen, A. Ali, I. C. Huang, J. S. Liu, P. Y. Chen, V. P. Viswanadha, C. Y. Huang, W. W. Kuo, Doxorubicin induced ROS-dependent HIF1α activation mediates blockage of IGF1R survival signaling by IGFBP3 promotes cardiac apoptosis. *Aging (Albany. NY).* **15**, 164–178 (2023).

36. C. Cui, Y. Pan, C. Zhang, D. Zhu, Y. Xuan, P. Hao, X. Ke, X. Zhou, Y. Qu, Eltrombopag binds SDC4 directly and enhances MAPK signaling and macropinocytosis in cancer cells - PubMed. *Am. J. Cancer Res.* **12**, 2697–2710 (2022).

37. H. Wang, H. Jin, A. C. Rapraeger, Syndecan-1 and syndecan-4 capture epidermal growth factor receptor family members and the α3β1 integrin via binding sites in their ectodomains: Novel synstatins prevent kinase capture and inhibitα6β4-integrindependent epithelial cell motility. *J. Biol. Chem.* **290**, 26103–26113 (2015).

38. A. de Laurentiis, L. Donovan, A. Arcaro, Lipid Rafts and Caveolae in Signaling by Growth Factor Receptors. *Open Biochem. J.* **1**, 12–32 (2007).

39. E. Bourseau-Guilmain, J. A. Menard, E. Lindqvist, V. Indira Chandran, H. C. Christianson, M. Cerezo Magaña, J. Lidfeldt, G. Marko-Varga, C. Welinder, M. Belting, Hypoxia regulates global membrane protein endocytosis through caveolin-1 in cancer cells. *Nat. Commun.* **7**, 11371 (2016).

40. J. Seong, M. Huang, K. M. Sim, H. Kim, Y. Wang, FRET-based Visualization of PDGF Receptor Activation at Membrane Microdomains. *Sci. Rep.* **7**, 1593 (2017).

41. U. Jo, K. H. Park, Y. M. Whang, J. S. Sung, N. H. Won, J. K. Park, Y. H. Kim, EGFR endocytosis is a novel therapeutic target in lung cancer with wild-type EGFR. *Oncotarget*. **5**, 1265–1278 (2014).

42. Y. Zhang, Y. Byun, Y. R. Ren, J. O. Liu, J. Laterra, M. G. Pomper, Identification of inhibitors of ABCG2 by a bioluminescence imaging-based high-throughput assay. *Cancer Res.* **69**, 5867–5875 (2009).

43. M. Archibald, T. Pritchard, H. Nehoff, R. J. Rosengren, K. Greish, S. Taurin, A combination of sorafenib and nilotinib reduces the growth of castrate-resistant prostate cancer. *Int. J. Nanomedicine*. **11**, 179–201 (2016).

44. Á. Telbisz, C. Hegedüs, A. Váradi, B. Sarkadi, C. Özvegy-Laczka, Regulation of the function of the human ABCG2 multidrug transporter by cholesterol and bile acids: Effects of mutations in potential substrate and steroid binding sites. *Drug Metab. Dispos.* **42**, 575–585 (2014).

45. R. J. Romanelli, T. L. Wood, Directing traffic in neural cells: Determinants of receptor tyrosine kinase localization and cellular responses. *J. Neurochem.* **105**, 2055–2068 (2008).

46. V. R. Dasari, V. Mazack, W. Feng, J. Nash, D. J. Carey, R. Gogoi, Verteporfin exhibits YAP-independent anti-proliferative and cytotoxic effects in endometrial cancer cells. *Oncotarget*. **8**, 28628–28640 (2017).

47. S. B. Jeong, R. Das, D. H. Kim, S. Lee, H. I. Oh, S. Jo, Y. Lee, J. Kim, S. J. Park, D. K. Choi, U. Y. Moon, O. bin Kwon, W. Namkung, S. Lee, B. C. Cho, J. Woo, Y. Seo, Anticancer effect of verteporfin on non-small cell lung cancer via downregulation of ANO1. *Biomed. Pharmacother.* **153**, 113373 (2022).

48. M. Yanagawa, M. Hiroshima, Y. Togashi, M. Abe, T. Yamashita, Y. Shichida, M. Murata, M. Ueda, Y. Sako, Single-molecule diffusion-based estimation of ligand effects on G protein-coupled receptors. *Sci. Signal.* **11**, eaao1917 (2018).

49. K. Kawakami, M. Yanagawa, S. Hiratsuka, M. Yoshida, Y. Ono, M. Hiroshima, M. Ueda, J. Aoki, Y. Sako, A. Inoue, Heterotrimeric Gq proteins act as a switch for GRK5/6 selectivity underlying β-arrestin transducer bias. *Nat. Commun.* **13**, 487 (2022).

50. D. T. Mcswiggen, H. Liu, R. Tan, S. A. Puig, L. B. Akella, R. Berman, M. Bretan, H. Chen, X. Darzacq, K. Ford, R. Godbey, A. Hanuka, A. Heckert, J. J. Ho, S. L. Johnson, R. Kelso, J. Li, K. Lin, B. Margolin, P. Mcnamara, L. Meyer, E. Sarah, A. Sule, Y. Tang, D. J. Anderson, H. P. Beck, High-throughput single molecule tracking identifies drug interactions and cellular mechanisms. *bioRxiv* (2023), doi:10.1101/2023.01.05.522916.

Acknowledgments:

We thank A. Kanayama for providing experimental support, P. Karagiannis for editing the manuscript, and all members of the Ueda lab for discussions. This project was supported by the Translational Science and Medicine Training Program, AMED, Center for Supporting Drug Discovery, Life Science Research, Osaka University, and the RIKEN Program for Drug Discovery and Medical Technology Platforms (DMP). **Funding:** AMED Grant Number JP22ym0126815, Japan; JST CREST Grant Number JPMJCR21E1, Japan; MEXT Grants-in-Aid for Scientific Research(B) (18H01839), Japan; MEXT Grants-in-Aid for Scientific Research(B) (22H02593), Japan; JSPS Grant-in-Aid for Scientific Research on Innovative Areas (18H05414), Japan. **Author contributions:** Conceptualization: MH and MU. Methodology: DW and MH. Investigation: DW and MH. Funding acquisition: MH and MU. Supervision: MU. Writing – original draft: DW, MH, and MU. Writing – review & editing: MH and MU. **Competing interests:** The authors declare no competing interests. **Data and materials availability:** Data availability: All data are available in the main text or the supplementary materials. All code used in the analysis are available from the authors upon reasonable request.

Figures

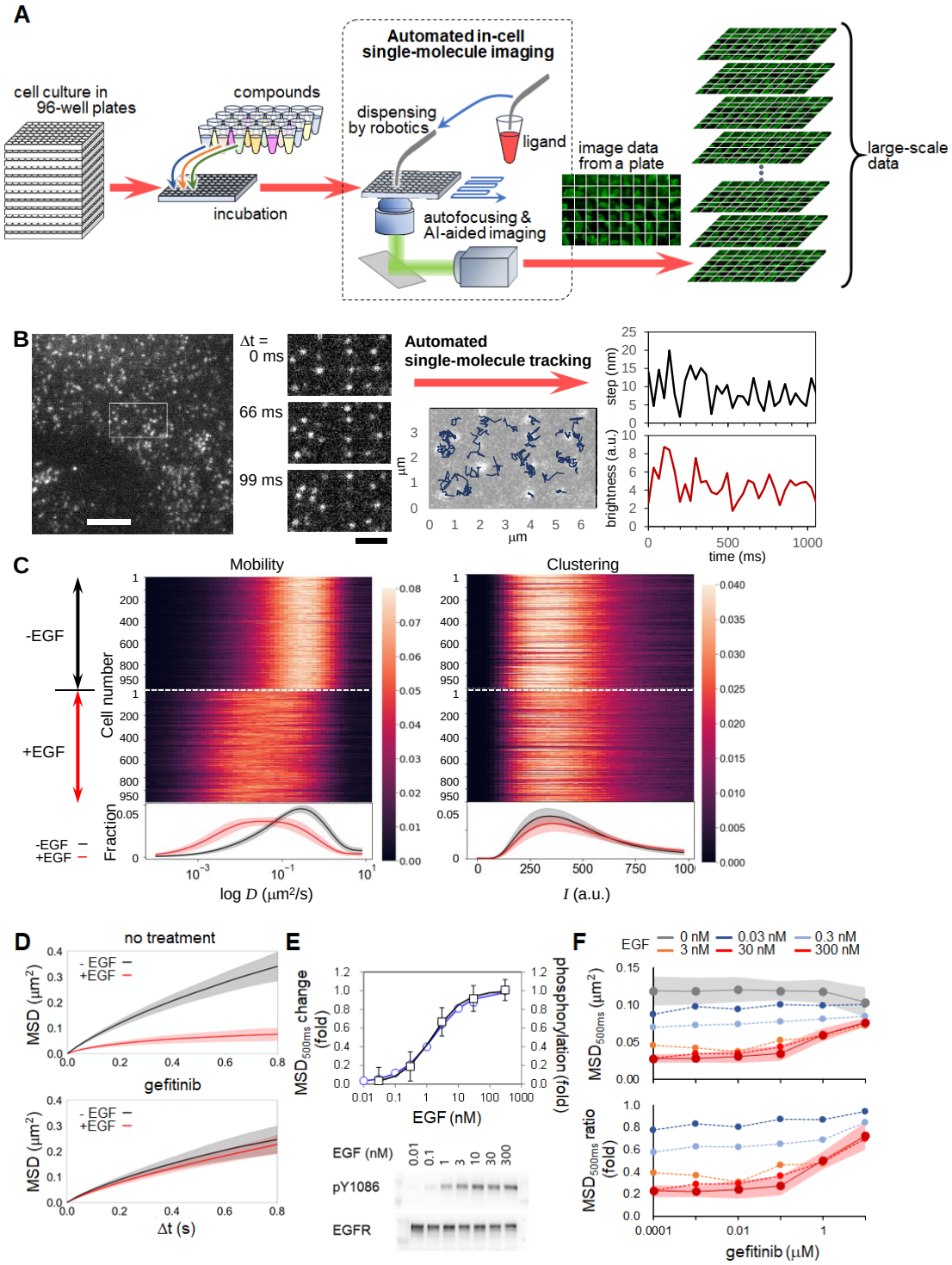

Fig. 1. Large-scale single-molecule imaging analysis of fluorescently labelled EGFR for drug screening.

(**A**) Schematic flow of single-molecule imaging using AiSIS for drug screening. (**B**) Automated single-molecule tracking. Left, representative images of EGFR-GFP observed with AiSIS. Scale bar, 5 μm. Middle left, time series images of the squared region in the left panel. Scale bar, 2 μm. Middle right, trajectories of EGFR (> 8 frames). Right, time series of step length (top) and brightness (bottom) of a spot in the left panels. (**C**) Heatmaps of diffusion coefficients and brightness corresponding to mobility and clustering, respectively. The average distributions over the cells are shown at the bottom. Black and red lines with shaded areas indicate the average with SD before and after EGF addition, respectively. (**D**) Time development of MSDs for either untreated or gefitinib-treated (10 μM) cells without (black) and with EGF (300 nM, red). **(E)** Relative changes in MSD_{500ms} and fold changes of phosphorylation obtained from western blotting (bottom) against different EGF concentrations. (**F**) Dose-dependency of gefitinib on MSD. Top, MSDs against gefitinib concentrations. Bottom, ratios between MSDs with and without EGF. Colored curves correspond to the indicated EGF concentrations. Shaded areas (C, D, and F) and error bars (E) indicate the SD and SE, respectively.

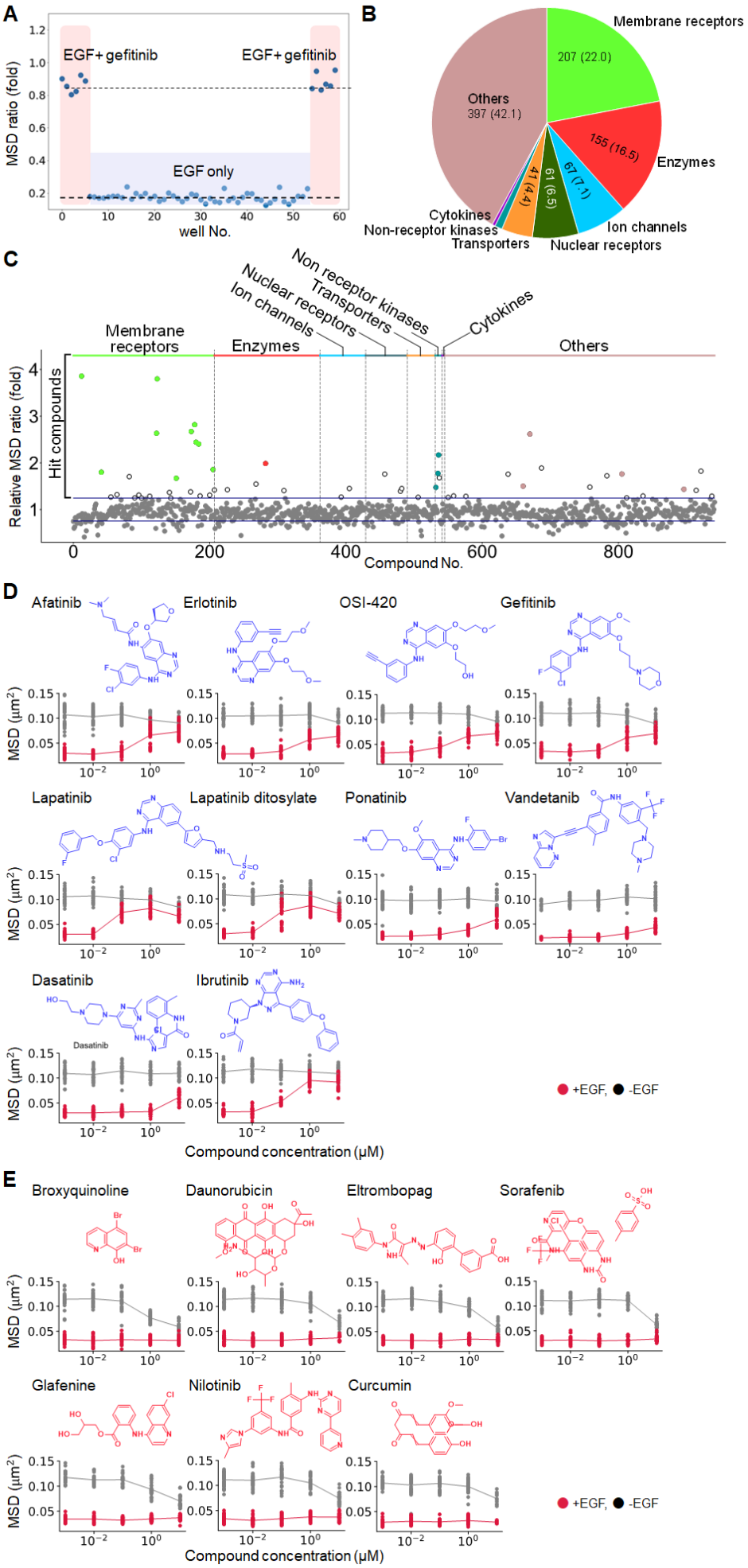
A
MSD ratio (fold)
EGF+gefitinib
EGF+gefitinib
EGF only
well No.
B
Membrane receptors
207 (22.0)
Others
397 (42.1)
155 (16.5)
Enzymes
67 (7.1)
61 (6.5)
41 (4.4)
Cytokines
Non-receptor kinases
Transporters
Nuclear receptors
Ion channels
C
Membrane receptors
Enzymes
Ion channels
Nuclear receptors
Transporters
Non receptor kinases
Cytokines
Others
Relative MSD ratio (fold)
Hit compounds
Compound No.
D
Afatinib
Erlotinib
OSI-420
Gefitinib
Lapatinib
Lapatinib ditosylate
Ponatinib
Vandetanib
Dasatinib
Ibrutinib
MSD (μm²)
+EGF, -EGF
Compound concentration (μM)
E
Broxyquinoline
Daunorubicin
Eltrombopag
Sorafenib
Glafenine
Nilotinib
Curcumin
MSD (μm²)
+EGF, -EGF
Compound concentration (μM)

Fig. 2. EGFR mobility-based screening for compounds in an FDA-approved library.

(**A**) Evaluation of single-molecule tracking as a screening method. MSD_{500ms} ratios of EGFR were calculated with and without gefitinib as positive and negative controls, respectively. Red-shaded regions indicate the MSD_{500ms} ratio obtained from wells treated with 30 nM EGF and gefitinib (positive control), and the blue-shaded region indicates wells treated with only EGF (negative control). (**B**) Target proteins of FDA-approved compounds in the library. (**C**) Effects of compounds on EGFR mobility were evaluated using the MSD_{500ms} ratio. Ratios for compound-treated cells were normalized to that for untreated cells. Blue lines denote upper and lower thresholds. The 53 hit compounds beyond the upper threshold are indicated by the colored and white circles. After further evaluation, the selected 18 compounds are denoted by colored circles, in which the colors indicate the type of target protein. (**D** and **E**) The dose-dependency was further evaluated by referring MSD_{167ms} against a series of compound concentrations. Red and black circles denote MSD values with and without EGF, respectively. 10 compounds (except auranofin) suppressed the EGF-dependent decrease in MSD (D), and 7 compounds reduced MSD regardless of EGF concentration (E).

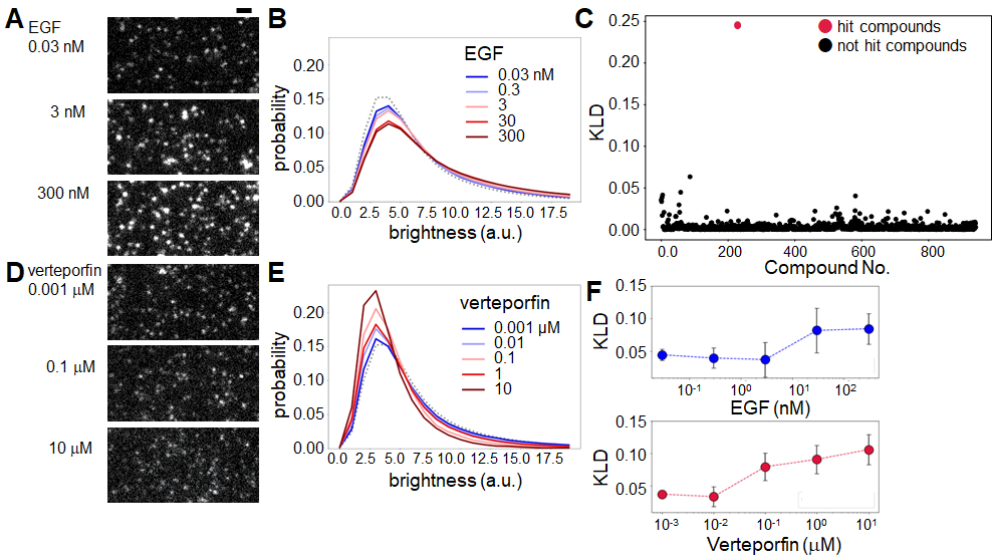

Fig. 3. EGFR clustering-based screening for compounds in the FDA-approved library.

(**A**) EGF facilitated the formation of EGFR oligomers. Single-molecule images of EGFR showed brighter and larger fluorescent spots were increased as the EGF concentration increased. Scale bar, 2 μm. (**B**) The probability distribution of EGFR spot brightness. EGFR fractions shifted from small to large oligomers with higher EGF concentration. (**C**) Effects of compounds on EGFR oligomerization were evaluated using the KLD of the brightness histograms before and after compound treatment. Verteporfin exhibited extremely high KLD values (red dot). (**D**) Verteporfin treatment increased the EGFR spots with lower brightness. (**E**) The probability distribution of EGFR spot brightness. The fraction of smaller EGFR oligomers was increased with verteporfin concentration, suggesting disassembly of the EGFR oligomers. (**F**) EGF (top) and verteporfin (bottom) dose-dependent KLD against the untreated condition. Error bars, SD.

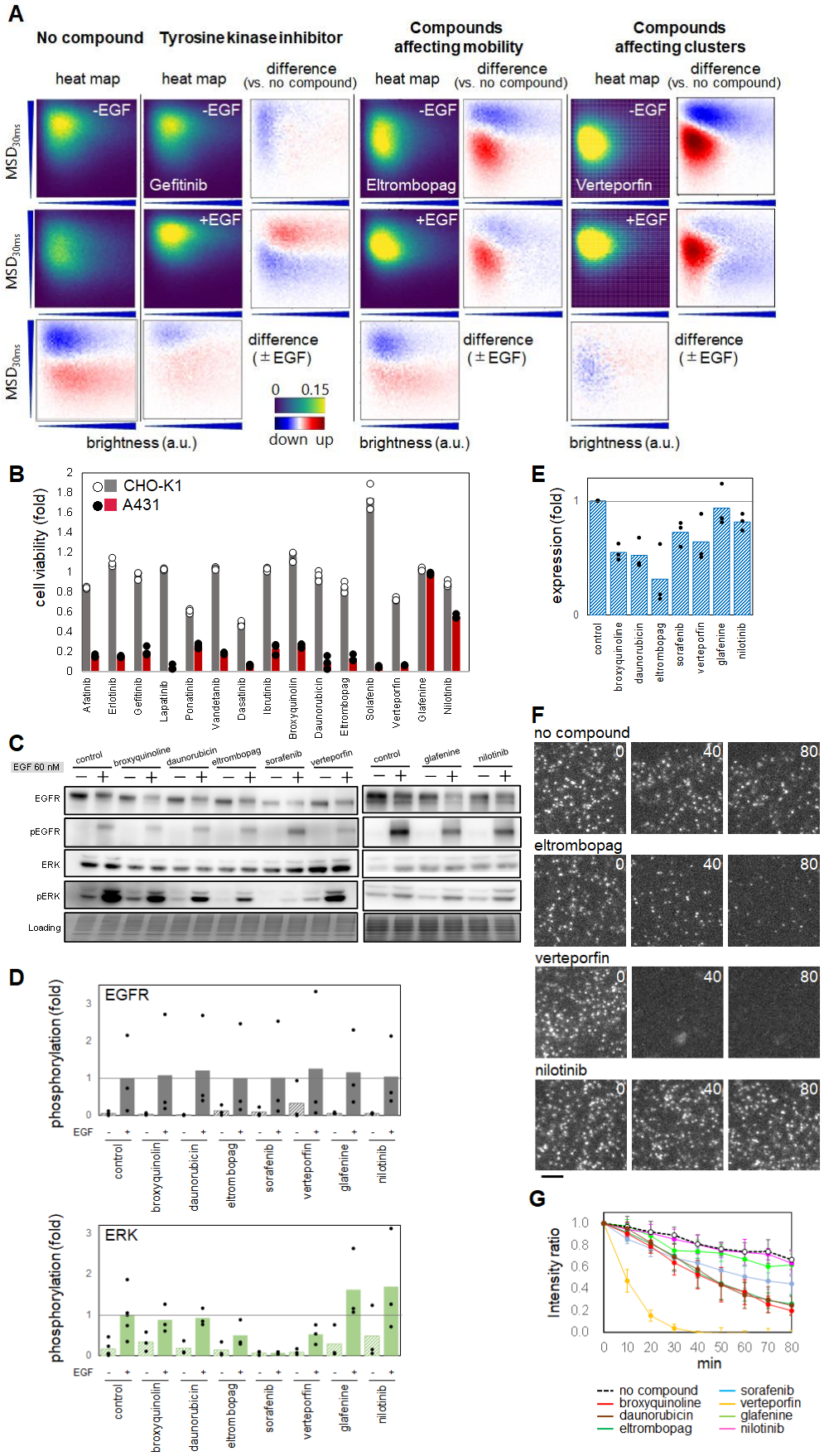
A
No compound
Tyrosine kinase inhibitor
Compounds affecting mobility
Compounds affecting clusters
heat map
difference (vs. no compound)
-EGF
+EGF
Gefitinib
Eltrombopag
Verteporfin
MSD30ms
difference (± EGF)
0 0.15
down up
brightness (a.u.)
B
CHO-K1
A431
cell viability (fold)
Afatinib
Erlotinib
Gefitinib
Lapatinib
Ponatinib
Vandetanib
Dasatinib
Ibrutinib
Broxyquinolin
Daunorubicin
Eltrombopag
Sorafenib
Verteporfin
Glafenine
Nilotinib
C
EGF 60 nM
control
broxyquinoline
daunorubicin
eltrombopag
sorafenib
verteporfin
glafenine
nilotinib
EGFR
pEGFR
ERK
pERK
Loading
D
EGFR
ERK
phosphorylation (fold)
EGF
E
expression (fold)
F
no compound
eltrombopag
verteporfin
nilotinib
0
40
80
G
Intensity ratio
min
no compound
broxyquinoline
daunorubicin
eltrombopag
sorafenib
verteporfin
glafenine
nilotinib

Fig. 4. Effects of compounds on EGFR behavior and cell responses.

(**A**) Heatmaps of EGFR mobility (MSD) and clustering (brightness) in cells treated with the indicated compounds. Yellow regions indicate higher frequency fractions. Differences between heatmaps with and without compound or EGF are mapped in red and blue for positive and negative values, respectively. (**B**) Viabilities of CHO-K1 (gray) and A431 (red) cells treated with the hit compound. Viabilities were normalized to untreated cells. (**C to E**) Phosphorylation of EGFR and its downstream signaling protein (C and D) and EGFR protein expression (C and E). After treatment with the indicated compounds for one hour (dashed bar), the cells were stimulated with EGF for 5 minutes (filled bar). Band densities were normalized to the unstimulated condition with EGF. Gray lines indicate phosphorylation and expression levels in untreated cells. (**F**) Timelapse single-molecule images acquired at 0, 40, and 80 min after the compound treatment. Scale bar, 3 μm (**G**). Quantified fluorescence per unit area, which was normalized to that at time 0. Solid lines correspond to the indicated compound. Black dotted lines denote the fluorescence of untreated cells exhibiting a decrease by bleaching. Error bars, SD.

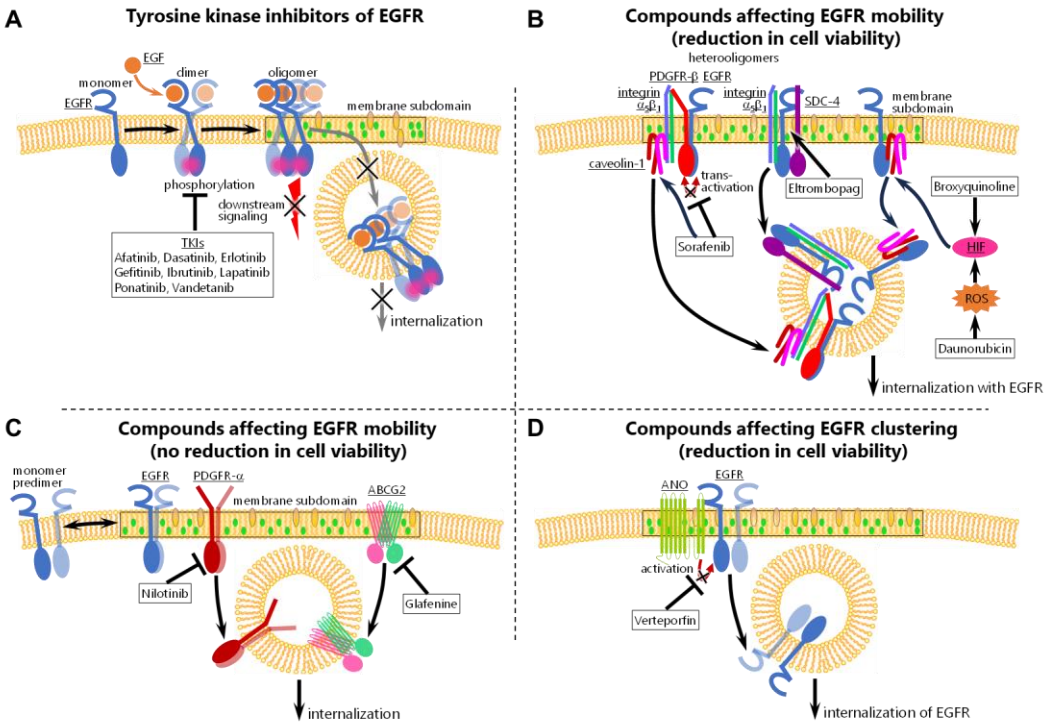

Fig. 5. Categorized schemes for effects of hit compounds on EGFR.

Possible schemes for the hit compounds. (**A**) TKIs suppress the EGF-induced phosphorylation of EGFR, thereby inhibiting the subsequent signaling process. (**B**) Compounds reducing both EGFR mobility and cell viability induce EGFR internalization with the target protein as a complex. (**C**) Compounds reducing EGFR mobility but without affecting cell viability internalize the target protein but not EGFR. (**D**) Compounds affecting EGFR clustering and cell viability facilitate EGFR internalization.